ESC European Society of Cardiology

Cardiovascular Research (2020) **116**, 1721–1732
doi:10.1093/cvr/cvz262

Blood flow patterns regulate PCSK9 secretion via MyD88-mediated pro-inflammatory cytokines

Shijie Liu[1,2†], Xiaoyan Deng[3,4†], Peng Zhang [3†], Xianwei Wang [2], Yubo Fan[3,4], Sichang Zhou[5], Shengyu Mu[6], Jawahar L. Mehta [2*], and Zufeng Ding[1,2*]

[1]College of Basic Medical Sciences, Henan Key Laboratory of Medical Tissue Regeneration, Xinxiang Medical University, Xinxiang, China; [2]Department of Internal Medicine, Central Arkansas Veterans Healthcare System and University of Arkansas for Medical Sciences, Little Rock, AR, USA; [3]Key Laboratory for Biomechanics and Mechanobiology of Ministry of Education, School of Biological Science and Medical Engineering, Beihang University, Beijing, China; [4]Beijing Advanced Innovation Center for Biomedical Engineering, Beihang University, Beijing, China; [5]Department of Neurological Surgery, Weill Cornell Medicine, New York, NY, USA; and [6]Department of Pharmacology and Toxicology, College of Medicine, University of Arkansas for Medical Sciences, Little Rock, AR, USA

Received 24 June 2019; revised 29 August 2019; editorial decision 23 September 2019; accepted 1 October 2019; online publish-ahead-of-print 7 October 2019

Time for primary review: 24 days

Aims Blood flow patterns play an important role in the localization of atherosclerosis in the sense that low-flow state is pro-atherogenic, and helical flow is protective against atherosclerosis. Proprotein convertase subtilisin/kexin type 9 (PCSK9) regulates cholesterol metabolism via low-density lipoprotein receptor (LDLr) degradation and is highly expressed in the atherosclerotic tissues. This study was designed to investigate the role of different blood flow patterns in the regulation of PCSK9 expression.

Methods and results We designed an experimental model guider to generate stable helical flow. Our data showed that compared with normal flow, low-flow state induces whereas helical flow inhibits PCSK9 expression in the rabbit thoracic aorta in an inflammatory state. Our data also identified that TLR4-MyD88-NF-κB signalling plays an important role in PCSK9 expression. On the other hand, TRIF pathway had almost no effect. Further studies showed that the signals downstream of NF-κB, such as pro-inflammatory cytokines (IL-1β, IL-18, MCP-1, IL-6, TNF-α, IL-12, IFNγ, and GM-CSF) directly influence PCSK9 expression. Interestingly, high fat diet further enhanced PCSK9 expression in an inflammatory milieu.

Conclusions These observations suggest a link between abnormal flow patterns and PCSK9 expression in inflammatory states, which may qualify helical flow and pro-inflammatory cytokines as potential targets to treat PCSK9-related cardiovascular diseases.

* Corresponding authors. Tel: (501) 257-4835; fax: (501) 257-4822, E-mail: zding@uams.edu (Z.D.); Tel: (501) 296-1426; fax: (501) 686-6180, E-mail: mehtajl@uams.edu (J.L.M.)

† These authors contributed equally to this work.

Graphical Abstract

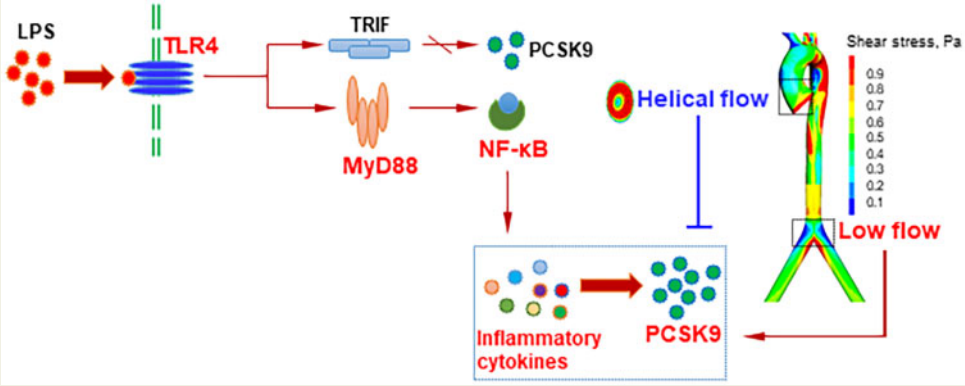

Keywords PCSK9 • helical flow • TLR4 • pro-inflammatory cytokines

1. Introduction

Local haemodynamic factors, especially blood flow induced wall shear stress, play an essential role in the development of atherosclerosis.[1] Shear stress patterns are determined by the direction and magnitude of blood flow.[2] For example, undisturbed laminar flow refers to smooth streamlined flow associated with high shear stress and disturbed flow at the site of arterial branch points or curvatures is associated with low shear stress. Steady laminar blood flow (associated with high shear stress) occurring in large straight segments of arterial bed is atheroprotective. Disturbed flow (associated with low shear stress) occurring at branch points and curvature permits accumulation of atherogenic particles and decreases the transport of anti-atherogenic oxygen from the blood to the arterial wall. Helical flow is seen in regions of ascending aorta that are twisted with a non-planar geometry, with helices on the aortic cross-sections and secondary rotations.[3] Helical flow has many positive physiological roles, such as eliminating areas of flow stagnation, preventing the accumulation of atherogenic lipids, and enhancing oxygen transport.[4]

Proprotein convertase subtilisin/kexin type 9 (PCSK9) plays a regulatory role in cholesterol homeostasis by promoting low-density lipoprotein receptor (LDLr) degradation. PCSK9 inhibition has emerged as a novel drug therapy to treat hypercholesterolaemia and related cardiovascular diseases.[5] Although the vast majority of the studies has focused on the role of PCSK9 in LDLr expression in the liver, an increasing body of evidence suggests that PCSK9 gene is also present in extra-hepatic tissues. Recent studies showed that PCSK9 is highly expressed in vascular endothelial cells,[6] smooth muscle cells,[7] and macrophages,[7,8] and its expression is regulated by many pro-inflammatory factors, such as lipopolysaccharide (LPS). Studies in atherosclerotic tissues show intense expression of PCSK9 in the affected regions,[9,10] raising the possibility that local PCSK9 expression may influence the development of atherosclerosis.

This study was designed to study the influence of various types of blood flow (normal flow, low flow, and helical flow) on PCSK9 expression along the aorta.

2. Methods

2.1 Helical flow guider design

A helical flow guider for the test vessels was fabricated to generate a stable helical flow in the test vessels. The guider had an axial length of 6.5 mm. The internal diameters of its inlet and outlet were 2 and 3 mm, respectively. The helical flow guider model was created using the computer-aided design software SolidWorks 2006. In order to meet the requirement of size and precision, the guider was fabricated using a photosensitive resin with laser rapid prototyping technology.

2.2 Model information

Normal flow (or low flow) and helical flow simulations were used wall-free geometries. To minimize the influence from outlet boundary conditions, straight extensions were set at the outlets, equalling to nine times the diameter of the vessel.

2.3 Mesh information

Computational meshes in the vessel model were carried out using ANSYS ICEM CFD (ANSYS Inc., Canonsburg, PA, USA). After an appropriate mesh independence investigation, the final volume meshes for the normal flow model and helical flow model were 782 789 and 1 316 523, respectively. In order to capture the velocity gradient in the boundary layer, high-density mesh elements were applied near the vessel walls, which specified with initial thickness in 0.001 mm and total thickness in 0.05 mm.

2.4 Governing equations

Flow simulations are based on the 3D incompressible Navier–Stokes and continuity equations:

$$\rho\left(\frac{\partial \mathbf{u}}{\partial t}+\mathbf{u}\cdot\nabla\mathbf{u}\right)=-\nabla p+\nabla\cdot\tau \quad (1)$$

$$\nabla\cdot\mathbf{u}=0 \quad (2)$$

where $\mathbf{u}$ and p represent the fluid velocity vector and pressure,

respectively. ρ is blood density ($\rho = 1060\,kg/m^3$) and τ denotes the stress tensor.

Blood was assumed to be an isotropic, incompressible, homogeneous, laminar, non-Newtonian fluid. The Carreau model was applied to calculate the blood viscosity.

2.5 Boundary condition

To ensure fully developed velocity profiles at the inlet, a parabolic inflow profile was used in the inlet cross-section, assuming Q_{inflow} = 3.3 mL/s based the experimental measurements. A rigid-wall no-slip boundary condition was implemented at the model walls. At the outlet, a specified pressure in 100 mmHg was applied as described previously.

2.6 Numerical scheme

The governing equations of blood flow were resolved by means of ANSYS FLUENT CFD (ANSYS Inc., Canonsburg, PA, USA), which used finite volume method. The SIMPLE algorithm was utilized for the pressure–velocity coupling. A coupled solver was performed with a second-order upwind scheme for the momentum spatial discretization. The convergence criterion was set to be 10^{-5} for both continuity and velocity residuals.

2.7 Animals and diets

Male New Zealand Rabbits (Laboratory Animal Center, Peking University, China) approximately 12 weeks old and weighing on average 3.0 ± 0.1 kg were kept as per the protocol approved by the institutional committee on animal use. All animal care complied with the 'Principles of Laboratory Animal Care' (NIH no. 85-23, revised 1985) and the 'Guide for the Care and Use of Laboratory Animals' (NRCC, 8th edition, revised 2011). Rabbits were reared in rooms under natural conditions with an ambient temperature ranged from 25°C to 28°C and relative air humidity at 50%. A 12 h light to12 h dark cycle was used throughout the study. All rabbits were allowed to acclimatize for 1 week, and then were divided into four groups ($n = 7$) and fed standard rabbit diet or high fat diet (HFD; prepared with mixing standard diet (SD) with extra 15% fat, by fortifying with corn oil and lard, in a ratio of 2:1), the experimental period lasted 12 weeks. To induce an inflammatory condition, LPS at 10 μg/kg was administered intravenously every 3 days.

2.8 Preparation of arterial segments

Rabbits were anaesthetized with a mixture of xylazine (2.5 mg/kg) and ketamine (25 mg/kg) given through the right marginal ear vein. Cannulae were then advanced approximately 2 mm into the each end of the aorta, enabling their tips to lay beyond any regions liable to have been damaged during the excision procedure. After a ligature was tied around each cannula as close to the tip as possible, the cannulated vessel was dissected from the body. Aortas were flushed slowly to wash out any remaining blood. In order to minimize damage to the endothelium, the aorta was pressurized throughout the experiment by a reservoir placed 1.0 m above the artery and filled with Krebs–Henseleit solution. The aorta was thoroughly examined for leakage *in situ* by pressing the aorta; any points on the aorta that leaked were sealed by coagulation with an electrical fulgurator. During the entire process, Krebs–Henseleit solution was constantly applied to the outer surface of the aorta to prevent it from drying.

2.9 Perfusion solution and perfusion system

For each experiment, cell culture medium 1640 containing foetal calf serum (FBS, 10%), penicillin (100 IU/mL), and streptomycin (100 mg/mL; Sigma, St Louis, MO, USA) was freshly prepared as the experimental perfusion solution, in which chemical inhibitors or peptides (2 h prior to LPS treatment) were added for another 12 h. The pH value of the perfusion solution was adjusted to 7.2.

Figure 1F shows a schematic drawing of the experimental perfusion system. It consisted of a head tank, a downstream collecting reservoir, a peristaltic flow pump with flow meter (FH100; Thermo Fisher Scientific) to circulate the perfusion fluid (1640, cell culture medium) and a blender of air and CO_2 with a constant temperature at 37°C. All of the components of the perfusion system were connected using tygon tubing. The flow rate was controlled by adjusting peristaltic pump. The harvested artery with the metal frame was immersed in Krebs–Henseleit solution and then connected horizontally to the perfusion system.

2.10 Treatment with chemical inhibitors or specific inhibitor peptide set, and recombinant rabbit proteins

To investigate the role of TR4 pro-inflammatory cytokines signalling in regulation of PCSK9 expression, different inhibitors, peptide sets, or recombinant proteins were used as follows.

2.10.1 In vitro

Prior 2 h treatment with LPS at 20 ng/mL, the following inhibitors were treated: TLR4 inhibitor TAK-242 (Millipore, Burlington, MA, USA) at 1 μM, TLR4 Inhibitor Peptide Set at 100 μM (Novus Biologicals, Littleton, CO, USA); MyD88 inhibitory peptide Pepinh-MYD at 20 μM (InvivoGen, San Diego, CA, USA), MyD88 Inhibitor Peptide Set at 100 μM (Novus Biologicals, Littleton, CO, USA); TRIF inhibitory peptide Pepinh-TRIF at 40 μM (InvivoGen, San Diego, CA, USA), TRIF monoclonal antibody at 1 μg/mL (Novus Biologicals, Littleton, CO, USA); NF-κB inhibitors BAY 11-7085 at 10 μM and Helenalin at 10 μM (Santa Cruz, Dallas, TX, USA). Control for chemical inhibitors: DMSO; Control for the peptide: specific control peptide.

2.10.2 In vivo

In HFD group, prior 2 h to LPS injection, the following inhibitors were injected: TLR4 inhibitor TAK-242 at 2 mg/kg body weight, MyD88 inhibitory peptide Pepinh-MYD at 1 mg/kg body weight, TRIF inhibitory peptide Pepinh-TRIF at 1 mg/kg body weight, and NF-κB inhibitor Helenalin at 5 mg/kg body weight.

Recombinant rabbit proteins were treated as indicated concentration under normal flow for 12 h: IL-1β (Cat. ab209157, Abcam, Cambridge, MA, USA) at 4 ng/mL, IL-18 at 50 ng/mL (Cat. MBS2030884, MyBioSource, San Diego, CA, USA), MCP1 at 100 ng/mL (Cat. ab151202, Abcam, Cambridge, MA, USA), IL-6 at 20 ng/mL (Cat. RP1281U-100, Kingfisher Biotech, Saint Paul, MN, USA), TNF-α at 50 ng/mL (Cat. 5670-TG-025/CF, Novus Biologicals, Littleton, CO, USA), IL-12 at 10 ng/mL (Cat. GR104270, Genorise Scientific, Glen Mills, PA, USA), IFN-γ at 10 ng/mL (Cat. ab93911, Abcam, Cambridge, MA, USA) and GM-CSF at 2 ng/mL (Cat. ab209131, Abcam, Cambridge, MA, USA).

2.11 Enzyme-linked immunosorbent assay

Secretion of PCSK9, IL-1β, MCP-1, IL-6, TNFα, IL-12, and IFNγ was measured in rabbit sera or aorta by using a rabbit enzyme-linked immunosorbent assay (ELISA) kit for PCSK9, IL-1β, IL-18, MCP-1, IL-6, TNFα, IL-12,

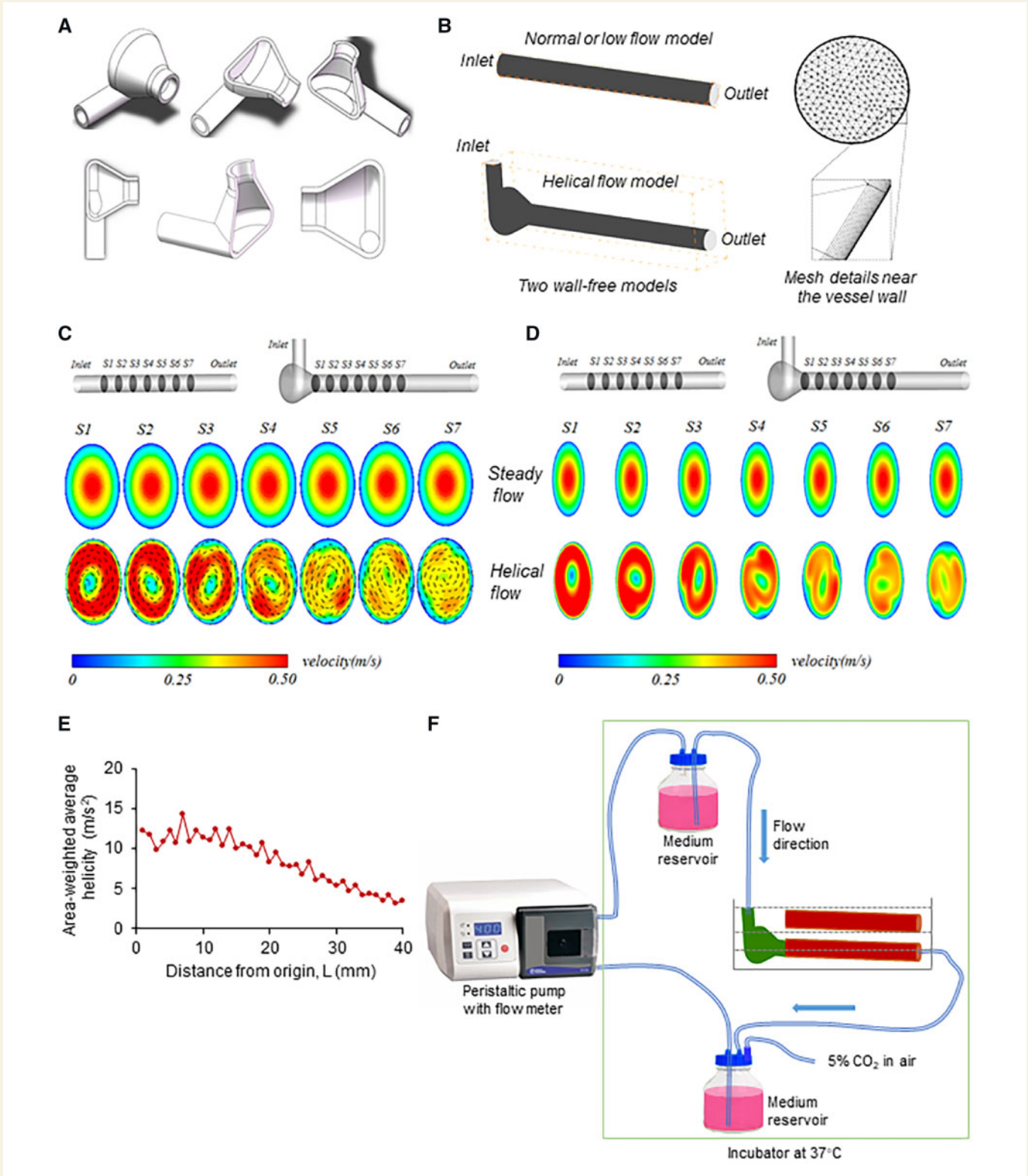

Figure 1 Helical flow and flow system. (*A*) Helical flow guider. (*B*) Flow models and mesh details near the vessel wall. (*C*, *D*) Velocity with or without vector under normal flow and helical flow. (*E*) The area-weighted average of helicity along the vessel. (*F*) Schematic drawing of the experimental perfusion system. The medium reservoir provides a steady flow in the thoracic aortic segment.

IFNγ, and GM-CSF (MyBioSource, Inc., San Diego, CA, USA); Rabbit ELISA kit for IL-18 and GM-CSF were from LSBio (Seattle, WA, USA).

2.12 Western blot

Protein aorta were purified with RIPA Lysis Buffer System (Santa Cruz, CA, USA) and loaded onto 12% Mini-PROTEAN® TGX™ Precast Gel (Bio-Rad, CA, USA) for electrophoresis. The size-separated proteins were then transferred to Hybond ECL Nitrocellulose Membranes (GE Healthcare, NJ, USA). After blocking with 5% BSA buffer for 1 h, the membranes were incubated with primary antibody at 1:3000 dilution overnight at 4°C. After washing with PBS containing 0.1% Tween-20, membranes were incubated with secondary antibody for 1 h and signals were detected with Pierce ECL Western Blotting Substrate (Thermo Scientific, IL, USA). Intensity quantification of the bands was obtained with Image J software and normalized to β-actin. Antibody directed at PCSK9 was from Biocompare (South San Francisco, CA, USA).

2.13 Real-time quantitative polymerase chain reaction

Total RNA was reverse transcribed at 42°C with SuperScript II (Life Technologies). Relative mRNA levels for each sample were quantified based on Ct (the amplification cycle threshold) normalized to GAPDH as an endogenous mRNA standard. Rabbit primers (Applied Biosystems) used were as follows: PCSK9 rabbit- Forward 5′-aggcacaggctgatccacttct-3′ Reverse 5′-agcagcccaacaactcctcatc-3′; LDLR rabbit- Forward 5′-caaa-gagtgcgcgaccaatgagtgc-3′ Reverse 5′-tcgtgccggttggtgaagaagaggta-3′; GAPDH rabbit- Forward 5′-ggccgcccagaacatcatcc-3′ Reverse 5′-gccagccccagcatcgaaggtagag-3′.

2.14 Statistical analysis

Data are presented as means ± standard deviation, representative of five rabbit per genotype ($n = 5$ with experiments *in vitro*) or seven rabbit per genotype ($n = 7$ with experiments *in vivo*) from three independent experiments. The significances between two groups were tested by unpaired *t*-test. Multiple comparisons were analysed by one-way ANOVA, followed by Tukey's *post hoc* comparisons test. Statistical analysis was performed with GraphPad Prism 7.00 (GraphPad Software, La Jolla, CA, USA). *P*-values of <0.05 were considered to be statistically significant.

3. Results

3.1 General flow pattern and helicity

First, we created an experimental model guider to generate stable helical flow (*Figure 1A*). *Figure 1B* show the model of normal, low, and helical flow as well as mesh details near the vessel wall. *Figure 1C, D* shows the flow patterns (velocity vectors at seven sections along the vessels) obtained numerically for the normal flow group and the helical flow group. As evident from the figure, helical flow was spiral. Note that there was no spiral flow in the normal flow group. The numerical simulation revealed that when compared with the normal flow group, the velocity profile in the helical flow shifted away from the tube centre in the helical flow group. The simulation also revealed that the spiral flow created by the flow guider was attenuated progressively along the vessel.

In order to better characterize the flow in the helical flow model, helicity was defined by the following equation:

$$H = (\nabla \times \vec{V}) \cdot \vec{V}$$

Figure 1E shows the area-weighted average of helicity of the flow at different cross-sections along the vessel. Helicity, indicator of the intensity of helical flow, created by the flow guider is the highest at the origin of the test vessel, and it decreases along the vessel and drops drastically at 10 mm from origin.

Based on this simulation, the flow system shown in *Figure 1F* was used in the following experiments.

3.2 Blood flow patterns regulate PCSK9 expression mediated by TLR4 signalling

To investigate the influence of different types of blood flow on PCSK9 expression, normal flow (steady laminar shear stress at 12 dynes/cm^2), low flow (steady laminar shear stress at 3 dynes/cm^2), and helical flow (same flow rate as normal flow) were applied in the straight segment of the rabbit thoracic aorta (length: 2.1 cm). As shown in *Figure 2A, B*, compared with normal flow, low-flow state resulted in enhanced PCSK9 expression (both mRNA and protein). Consistent with the data in *Figure 1E*, helical flow resulted in inhibition of PCSK9 expression in the first 0.9 cm from the start point, then PCSK9 expression increased gradually along the thoracic aorta as helical flow decreased progressively, and reached a constant value at 1.5 cm, when it became same as the corresponding value in the normal flow.

PCSK9 promotes LDLr intracellular degradation and contributes to development of atherosclerosis, we therefore investigated if blood flow-mediated PCSK9 expression determines LDLr degradation along the aorta. Our observations indicated that compared with normal flow, low-flow state inhibited LDLr expression whereas helical flow highly enhanced LDLr expression (both mRNA and protein) in the first 0.9 cm from start point (*Figure 2C, D*). These observations suggest that PCSK9 expression regulates LDLr expression in the arterial segments in states of altered flow, and PCSK9 and LDLr expression are inter-twined.

TLR4 is a member of the toll-like receptor (TLR) family that triggers innate immune responses to defend against invading microorganisms. TLR4 recognizes LPS and is the only known TLR that is able to activate both MyD88- and TRIF signalling, in the induction of pro-inflammatory cytokines and type I interferon, respectively.[11] We and others have shown that LPS is a powerful inducer of PCSK9 in endothelial cells, smooth muscle cells, and macrophages.[6–10] Here, we posited that TLR4 signalling may play an important role in LPS-mediated PCSK9 expression under different flow conditions. To test this hypothesis, several inhibitors of TLR4, MyD88, TRIF, and NF-κB were applied.

As helical flow significantly inhibits PCSK9 expression in the length between 0 and 0.6 cm, we used these sections to study the following experiments from *Figure 3A* to *Figure 3D*.

TAK-242 is a small-molecule inhibitor of TLR4 signalling. It inhibits the production of LPS-induced inflammatory factors by binding to the intracellular domain of TLR4.[12] As shown in *Figure 3A*, TAK-242 as well as specific TLR4 inhibitor peptide set significantly inhibited PCSK9 expression in states of normal flow, low flow, and helical flow. Treatment with the MyD88 inhibitor Pepinh-MYD and its specific inhibitor peptide set also markedly reduced PCSK9 expression (*Figure 3B*). In contrast, treatment with TRIF inhibitor Pepinh-TRIF and its antibody had almost no effect on PCSK9 expression (*Figure 3C*). As TRIF is not involved in LPS-induced PCSK9 expression, we focused only on TLR4-MyD88 signalling. NF-κB is a downstream signal in the TLR4-MyD88 pathway and regulates LPS-induced pro-inflammatory cytokines secretion.[13] As shown in *Figure 3D*, treatment with two different NF-κB inhibitors Bay11-7085

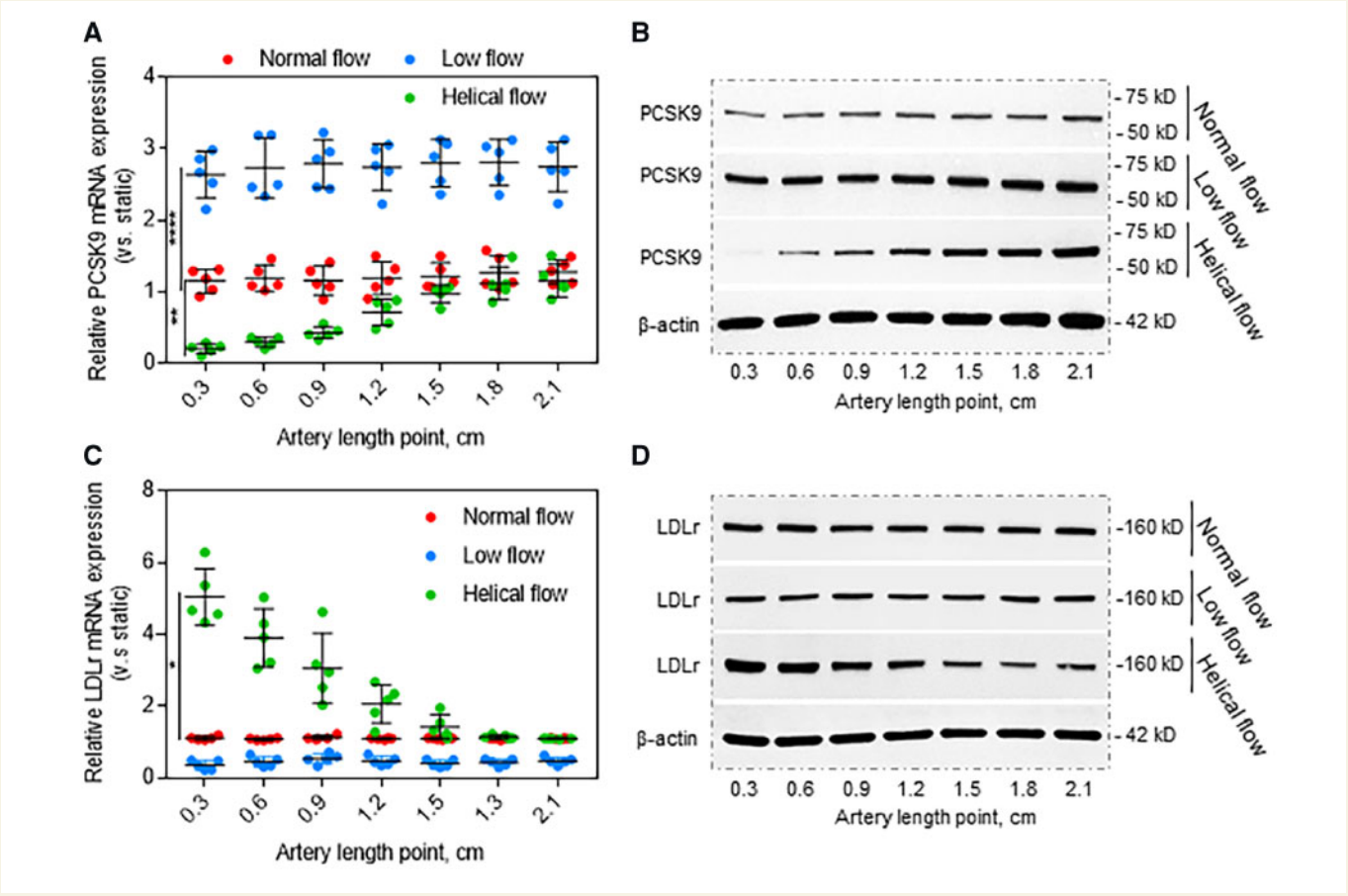

Figure 2 Flow patterns regulate PCSK9 expression. (*A*, *B*) Compared with normal flow, helical flow inhibits whereas low flow induces PCSK9 expression at both mRNA and protein levels. (*C*, *D*) Helical flow up-regulates whereas low flow down-regulates LDLr expression. The straight segments of the rabbit thoracic aorta were used in (*A*) to (*D*), treated with LPS (20 ng/mL) in the perfusion medium for 12 h. Bar graphs represent data compiled from three independent experiments ($n = 5$ rabbit per genotype), shown as mean ± standard deviation. The significances between two groups were tested by unpaired *t*-test; Multiple comparisons were analysed by one-way ANOVA, followed by Tukey's *post hoc* comparisons test (*$P < 0.05$, **$P < 0.01$; ****$P < 0.0001$).

and Helenalin markedly decreased PCSK9 expression. Of note, compared with the normal flow group, PCSK9 expression was the lowest in helical flow group whereas it was highest in the low-flow group.

3.3 PCSK9 distribution along the aorta of rabbits fed HFD

HFD pre-disposes to development of atherosclerosis. To investigate if HFD would influence PCSK9 expression in sites destined to develop atherosclerotic sites, rabbits were fed SD or HFD for 12 weeks. Saline or LPS (10 μg/kg) were given intravenously to rabbits every 3 days.

First, we confirmed that LPS in a dose of 10 μg/kg every 3 days had no effect on the survival of rabbits during the 12 weeks period (*Figure 4A*). The PCSK9 levels in serum were highest at 3 days, and gradually decreased from days 4 to 8, then stabilized subsequently (*Figure 4B*). Next, we observed that LPS significantly enhanced PCSK9 levels in serum in both SD and HFD-fed groups; but PCSK9 levels were much higher in HFD-fed rabbits compared with SD-fed group (*Figure 4C*).

As PCSK9 was highest on day 3 with LPS treatment, we chose this time point for subsequent experiments (*Figure 4E–G*).

Figure 4D is a schematic diagram of different sections of aorta showing different flow patterns along its length. Shear stress is low and flow is disturbed at the aortic branch points and aorta–iliac bifurcation.[14] In thoracic aorta and iliac arteries, shear stress is high and blood flow is relatively steady.[15] In the ascending aorta, shear stress is high and blood flow is helical.[16] As shown in *Figure 4E*, PCSK9 secretion was higher in all regions of aorta in LPS-treated animals, and were highest in aortic branch points and in the aorto–iliac bifurcation compared with the saline-treated control group ($P < 0.0001$). Of note, PCSK9 secretion was near normal or low in regions of helical flow (vs. thoracic aorta). It is also of note that PCSK9 secretion was similar in the regions of aorta when the animals had been given saline, and the differences became evident when the animals had been given LPS.

Consistent with these data, LDLr expression in LPS-treated group was much lower at aortic branch points, thoracic aorta, aorto–iliac bifurcation and iliac artery than in the ascending aorta (*Figure 4F*). But no difference in the ascending aorta. ELISA analysis for PCSK9 and pro-inflammatory cytokines (IL-1β, IL-18, MCP-1, IL-6, TNFα, IL-12, IFNγ, and GM-CSF) showed that LPS markedly induced PCSK9 and the pro-inflammatory cytokines (*Figure 4G*).

Separate groups of rabbits were administered TLR4 inhibitor TAK-242, MyD88 inhibitor Pepinh-MYD, TRIF inhibitor Pepinh-TRIF, and

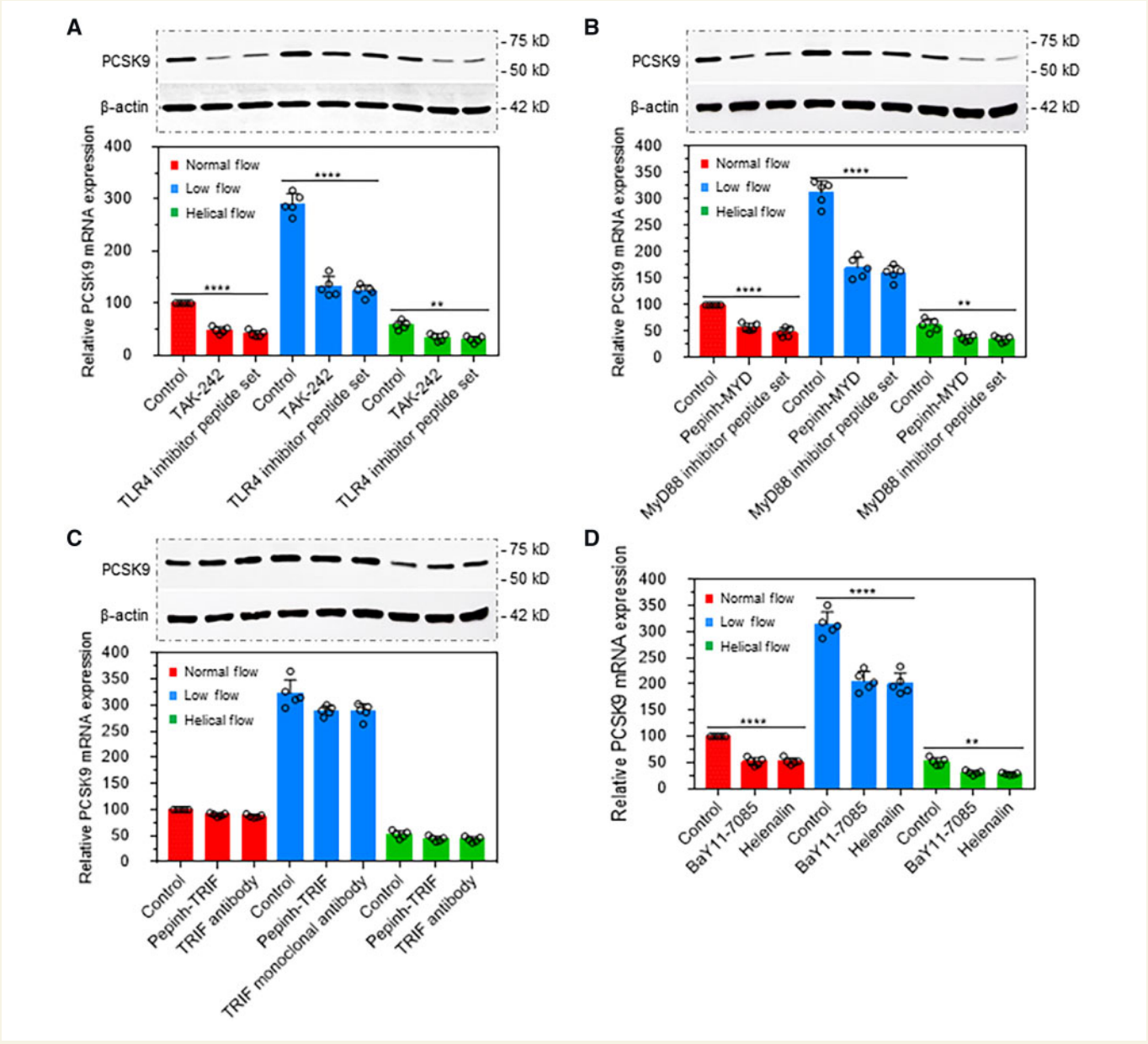

Figure 3 TLR4 signalling is involved in flow pattern-mediated PCSK9 expression. (*A*) TLR4 inhibitor TAK-242 and its specific inhibitor peptide decrease PCSK9 expression at both protein (upper panel) and mRNA level (lower panel). (*B*) MyD88 inhibitor Pepinh-MYD and its specific inhibitor peptide decrease protein and mRNA expression of PCSK9. (*C*) TRIF inhibitor Pepinh-TRIF and its monoclonal antibody almost have no effect on PCSK9 expression at both protein and mRNA level (lower panel). (*D*) NF-κB inhibitors BaY11-7085 and Helenalin decrease PCSK9 expression. The rabbit thoracic aorta with length points between 0 and 0.6 cm were used in (*A*) to (*D*), treatment with LPS at 20 ng/mL in the perfusion medium for 12 h. Bar graphs represent data compiled from three independent experiments ($n = 5$ rabbit per genotype), shown as mean ± standard deviation. The significances between two groups were tested by unpaired *t*-test; Multiple comparisons were analysed by one-way ANOVA, followed by Tukey's *post hoc* comparisons test (*$P < 0.05$, **$P < 0.01$; ****$P < 0.0001$).

NF-κB Helenalin to investigate the role of TLR4-MyD88-TRIF-NF-κB signalling in PCSK9 expression along the aorta prior to administration of LPS. As shown in *Figure 5A*, administration of TAK-242, Pepinh-MYD, and Helenalin significantly reduced PCSK9 expression along the aorta. Pepinh-TRIF treatment, on the other hand, had no effect on PCSK9 expression.

On the basis of the aforementioned data, it can be concluded that TLR4-MyD88-NF-κB signalling pathway plays a key role in the regulation of PCSK9 expression, particularly when the animals are given a potent inflammatory stimulus LPS. NF-κB translocation induces expression of various pro-inflammatory genes, and plays a critical role in regulating the survival, activation, and differentiation of innate immune cells and inflammatory T cells.[17]

As expected, LPS treatment induced an increase in all pro-inflammatory cytokines (IL-1β, IL-18, MCP-1, IL-6, TNFα, IL-12, IFNγ, and GM-CSF) measured in the serum (*Figure 5B*).

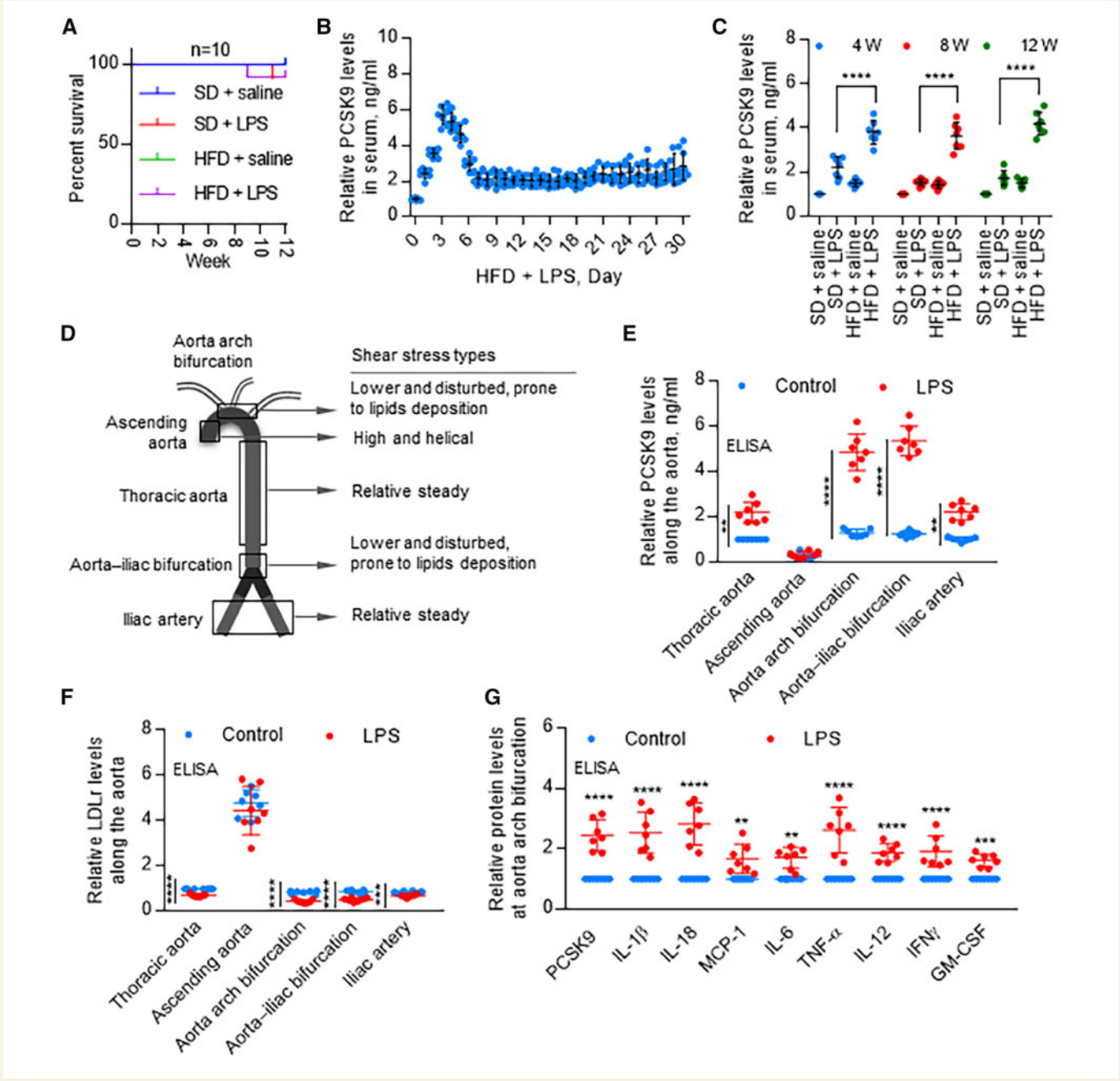

Figure 4 Distribution of PCSK9 expression along the aorta. (*A*) Rabbit survival rate in different groups with or without LPS treatment. (*B*) In HFD groups, PCSK9 levels in first 30 days after LPS treatment. Data were normalized to HFD + saline, set control HFD + LPS = 1 (0 day). (*C*) LPS treatment significantly induces serum PCSK9 levels in both SD and HFD groups, measured by ELISA at 4, 8, and 12 weeks. (*D*) Schematic drawing of flow patterns along the aorta. (*E*) PCSK9 levels along the aorta with or without LPS treatment on day 3 HFD, measured by ELISA. LPS induces PCSK9 expression in thoracic aorta, aorta arch branch points, aorta–iliac bifurcation, and iliac artery but not in ascending aorta. PCSK9 levels are highest in aortin arch branch points and aorta–iliac bifurcation. (*F*) ELISA analysis of LDLr expression along the aorta with or without LPS treatment on day 3 HFD. (*G*) ELISA analysis for expression of PCSK9 and pro-inflammatory cytokines at aorta arch bifurcation on day 3 HFD, set control without LPS = 1 in each group. Bar graphs represent data compiled from three independent experiments ($n = 7$ rabbit per genotype), shown as mean ± standard deviation. The significances between two groups were tested by unpaired *t*-test; Multiple comparisons were analysed by one-way ANOVA, followed by Tukey's *post hoc* comparisons test (**$P < 0.01$; ****$P < 0.0001$).

3.4 Pro-inflammatory cytokines induce PCSK9 expression

To clarify the role of the pro-inflammatory cytokines in the induction of PCSK9 expression, under normal flow condition of 12 dynes/cm^2, straight segments of the rabbit thoracic aorta were treated with recombinant IL-1β, IL-18, MCP-1, IL-6, TNF-α, IL-12, IFNγ, and GM-CSF. Each of these pro-inflammatory cytokines induced a several-fold increase in PCSK9 expression in aortic segments (*Figure 6A*). Importantly, low-flow

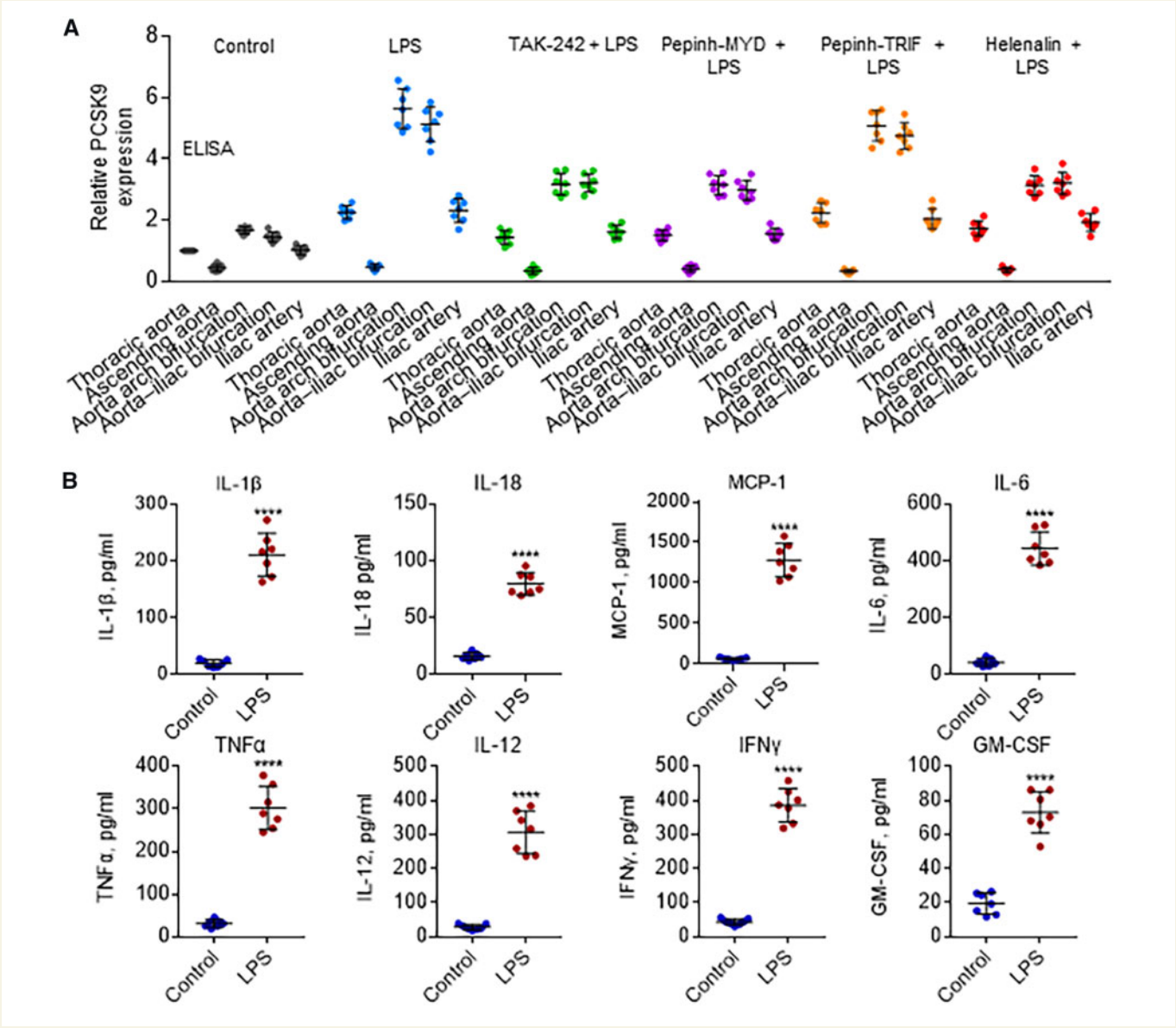

Figure 5 TLR4 signalling regulates distribution of PCSK9 expression along the aorta. (*A*) Effect of TLR4 inhibitor TAK-242, MyD88 inhibitor Pepinh-MYD, TRIF inhibitor Pepinh-TRIF, and NF-κB Helenalin on PCSK9 levels, measured by ELISA. (*B*) LPS injection induces expression of pro-inflammatory cytokines IL-1β, IL-18, MCP-1, IL-6, TNFα, IL-12, IFNγ, and GM-CSF. Measured by ELISA in serum on day 3 HFD group; rabbits treated with or without LPS. Bar graphs represent data compiled from three independent experiments ($n = 7$ rabbit per genotype), shown as mean ± standard deviation. The significances between two groups were tested by unpaired *t*-test; Multiple comparisons were analysed by one-way ANOVA, followed by Tukey's *post hoc* comparisons test (**$P < 0.01$; ****$P < 0.0001$).

regions showed a several-fold increase in the expression of a variety cytokines ($P < 0.0001$). On the other hand, regions with helical flow revealed a significant decrease in expression of each of these cytokines ($P < 0.02$; *Figure 6B*).

To confirm if pro-inflammatory cytokines directly induce PCSK9 expression, we focused on IL-1β, IL-6, TNF-α, and IFNγ and investigated their roles in regulation of PCSK9 expression in low-flow state. As shown in *Figure 6C*, IL-1β, IL-6, TNF-α, and IFNγ significantly induced PCSK9 expression. Concurrently, LDLr expression fell. We also confirmed that NF-κB was upstream of inflammatory cytokines (*Figure 6D*), because low-flow state induced and helical flow inhibited NF-κB expression compared with that of normal flow.

4. Discussion

Atherosclerosis generally develops in the regions of branch points and bifurcation, where blood flow is likely to be low and disturbed and shear stress to be high. On the other hand, regions with helical flow are relatively protected from deposition of atherosclerotic lipids and subsequent development of atherosclerosis.[1–4] Molecular mechanisms underlying these observations relative to the localization of atherosclerosis along the arterial bed remain unclear.

Previous studies have shown intense PCSK9 expression in atherosclerotic tissues from mice and humans.[7,10] *In vitro* studies have shown PCSK9 is highly expressed in aortic endothelial cells and smooth muscle

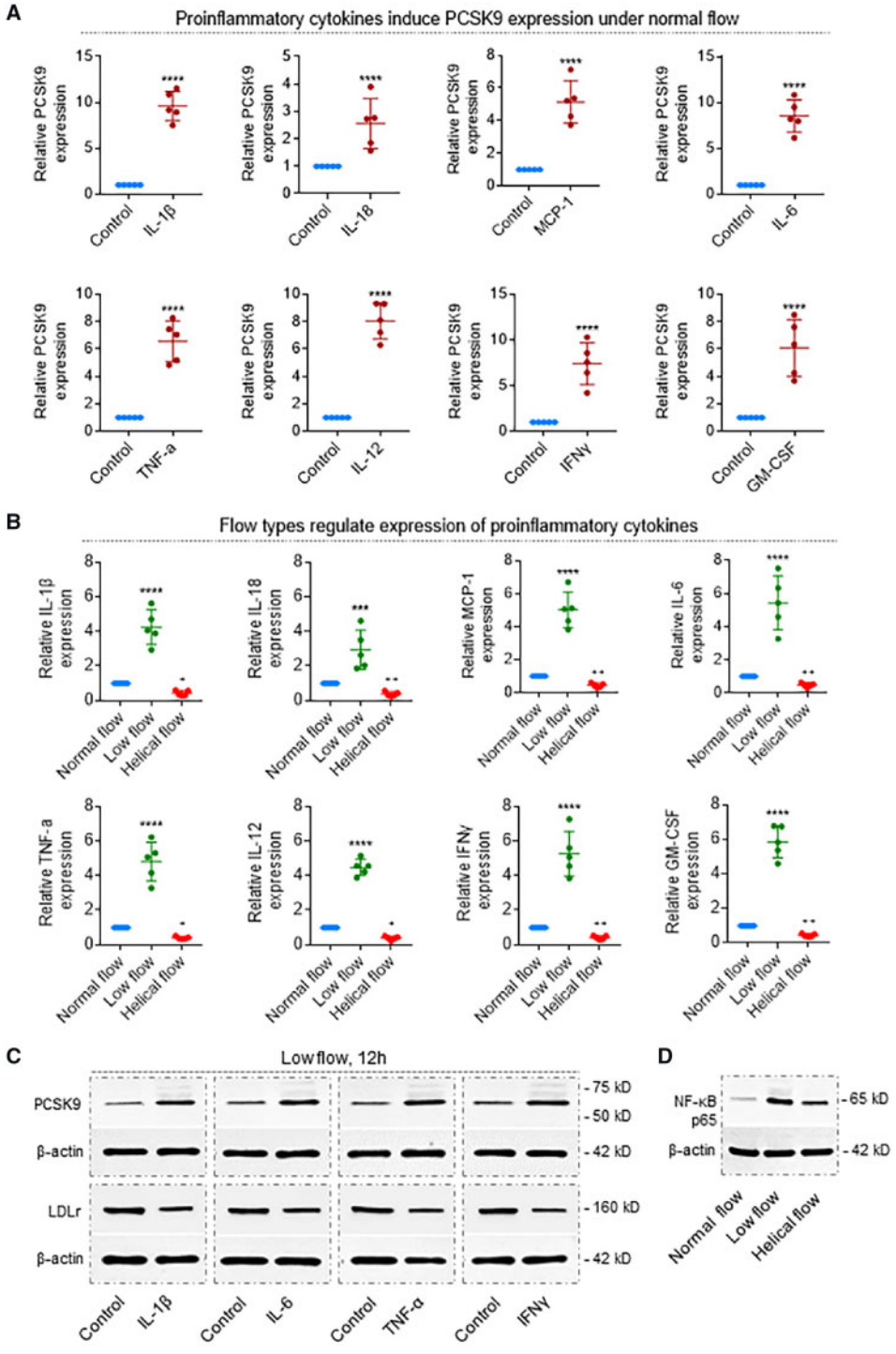

Figure 6 Pro-inflammatory cytokines determine PCSK9 levels, which is regulated by flow patterns. (*A*) Recombinant proteins IL-1β, IL-18, MCP-1, IL-6, TNFα, IL-12, IFNγ, and GM-CSF induce PCSK9 expression in the rabbit thoracic aorta. Recombinant proteins were added to the perfusion medium in different concentrations. Aortas were perfused for 12 h under normal flow conditions. ****$P < 0.0001$. Bar graphs represent data compiled from three independent experiments ($n = 5$ rabbit per genotype), shown as mean ± standard deviation. (*B*) Helical flow inhibits whereas low flow enhances LPS-induced release of pro-inflammatory cytokines: IL-1β, IL-18, MCP-1, IL-6, TNFα, IL-12, IFNγ, and GM-CSF. ****$P < 0.0001$ vs. normal group; $^{+}P < 0.05$, $^{+}P < 0.05$ vs. normal group, $^{++}P < 0.01$ vs. normal group. (*C*) Pro-inflammatory cytokines (IL-1β, IL-6, TNF-α, and IFNγ) regulate expression of PCSK9 and LDLr in the rabbit thoracic aorta. Aortas were perfused for 12 h under low-flow conditions, treatment with IL-1β at 4 ng/mL, IL-6 at 20 ng/mL, TNF-α at 50 ng/mL, and IFNγ at 10 ng/mL. (*D*) Flow types regulate NF-κB expression in the rabbit thoracic aorta. Aortas were perfused under low-flow conditions, treatment with LPS at 20 ng/mL in the perfusion medium for 12 h. Bar graphs represent data compiled from three independent experiments ($n = 5$ rabbit per genotype), shown as mean ± standard deviation. The significances between two groups were tested by unpaired *t*-test; Multiple comparisons were performed by one-way ANOVA, followed by Tukey's *post hoc* comparisons test.

cells, especially during a low-flow state.[6] The present studies revealed intense PCSK9 expression in regions with low flow, but low PCSK9 expression in regions with helical flow. These alterations in PCSK9 expression were identified when the arterial tissues were exposed to a small priming concentration of LPS *in vitro* and were subsequently confirmed in rabbits given LPS intravenously. These observations suggest a strong link between blood flow types and PCSK9 expression during an inflammatory state.

We created a helical flow model with internal diameters of 2 mm inlet and 3 mm at the outlet using a flow guider. This is the smallest diameter that can induce stable helical flow, evident from high helicity in the first 20 mm of the vascular segment. In the *in vitro* setting, we confirmed that different types of blood flow (steady normal flow, low flow, and helical flow) regulate PCSK9 expression. Next, in the *in vivo* setting, we showed differences in PCSK9 expression in different regions of aorta. PCSK9 expression became evident only after the segments of aorta were primed with small concentrations of LPS, as well as when the rabbits had been treated with a small non-lethal dose of the inflammatory stimulus LPS (10 μg/kg per 3 day). As expected the flow-mediated PCSK9 also modulated LDLr expression.

To clarify the role of dyslipidaemic state in PCSK9 regulation, rabbits were fed HFD for a period of 12 weeks. Again the survival rate of rabbits given small doses of LPS along with HFD was similar to that in rabbits given SD. Again, we observed that PCSK9 expression was highest in aortic branch points and aortic–iliac bifurcation where flow is disturbed and lowest in the aortic arch region where the flow is predominantly helical. Thus it appears that there is a marked variation in PCSK9 expression in different regions of aorta and this variation depends on the flow state. We showed that dyslipidaemia alone is a potent inducer for PCSK9 expression, especially under inflammatory conditions.

TLRs are required for pathogen recognition as part of the innate immune system. The TLRs regulate expression of pro-inflammatory cytokines and also the immune responses to infection. Among TLRs, TLR4 acts as a receptor for LPS and activates NF-κB to promote an inflammatory response.[18] In this study, we demonstrate a link between TLR4 and PCSK9 expression. With the use of a variety of inhibitors of different pathways of TLR4 signalling, we showed that TLR4-MyD88-NF-κB pathway, but not the TLR4-TRIF, is the key pathway in the regulation of PCSK9 expression along the aorta. Of note, LPS enhanced the serum levels of several pro-inflammatory cytokines, and treatment with recombinant proteins directed at these cytokines induced PCSK9 expression in the thoracic aorta.

It is generally believed that liver-secreted PCSK9 is the main source of circulating PCSK9, which degrades LDLr, leading to hyperlipidaemia. However, two significant contributors to atherosclerotic plaque progression are smooth muscle cells and macrophages in the media. Both smooth muscle cells and macrophages are not directly exposed to circulating PCSK9. We have shown that smooth muscle cells[6] and macrophages[8] secrete large amount of PCSK9 under inflammatory conditions. On the basis of this background, we believe that extra-hepatic PCSK9, particularly from vascular cells, may play a key role in the development of atherosclerosis. In addition, compared with native LDL, oxidized LDL (ox-LDL) contributes to foam cells formation and is an important event in atherogenesis. In a previous study,[8] we showed that in an inflammatory milieu elevated levels of PCSK9 stimulate the expression of SRs (principally LOX-1) and ox-LDL uptake in macrophages, and thus might contribute to the process of atherogenesis. In a complementary study, Liu and Frostegård[19] recently showed that PCSK9 plays a role in ox-LDL-induced dendritic cell maturation and activation of T cells from human blood and atherosclerotic plaque. This indicates that PCSK9 may have other functions besides LDLr degradation. Previously, we suggest that in keeping with a previous study,[20,21] it is the aortic torsion that induces helical flow in the aortic arch, which reduces PCSK9 secretion and the luminal surface LDL concentration in the aortic arch, protecting it from atherogenesis.

Besides ox-LDL, many modified LDL, e.g. acetylated LDL and aggregated LDL, may lead to foam cell formation.[22] Furthermore, LDL and very LDL can be atherogenic without lipoprotein modification.[21] However, no clinical study suggests that PCSK9 inhibition results in inhibition of clinically relevant endpoints independent of cholesterol lowering. Further studies need to be performed to clarify if PCSK9 can regulate uptake or accumulation of LDL, modified LDL and VLDL. As atherogenesis is the process of formation of plaques that often occurs in the intima layer of arteries, further studies need to be performed to clarify the importance of local vs. circulating PCSK9 concentrations.

Taken together, our results show that different flow types act as regulators for PCSK9 expression in an inflammatory milieu, via TLR4-MyD88-NF-κB pro-inflammatory cytokines signalling pathway. Our findings highlight helical flow and pro-inflammatory cytokines as critical regulators of PCSK9 secretion. We also anticipate that these findings will trigger future studies aimed at prevention of pro-inflammatory cytokines in treatment with PCSK9-related cardiovascular diseases.

Acknowledgements

Z.D. conceived the experiment, conducted experimental work, analysed data, and drafted the manuscript. J.L.M. drafted and revised the manuscript. X.D. and P.Z. designed helical flow guider and performed simulation experiments. Z.D., X.W., and S.L. performed experimental work. Y.F., Q.L., and S.Z. were responsible for resources and supervised the preclinical experiments. All authors reviewed and commented on the manuscript.

Conflict of interest: none declared.

Funding

This work was supported by National Natural Science Foundation of China (No. 11332003). Additional supported by National Natural Science Foundation of China (Nos. 11572028, 11421202); National Key Research and Development Program in China (No. 2016YFC1101100). Other support was provided by the Veterans Health Administration, Office of Research and Development, Biomedical Laboratory Research and Development (grant #BX000282-09A2 to Dr. Mehta).

References

1. Chatzizisis YS, Coskun AU, Jonas M, Edelman ER, Feldman CL, Stone PH. Role of endothelial shear stress in the natural history of coronary atherosclerosis and vascular remodeling: molecular, cellular, and vascular behavior. *J Am Coll Cardiol* 2007;**49**:2379–2393.
2. Chiu JJ, Chien S. Effects of disturbed flow on vascular endothelium: pathophysiological basis and clinical perspectives. *Physiol Rev* 2011;**91**:327–387.
3. Liu X, Sun A, Fan Y, Deng X. Physiological significance of helical flow in the arterial system and its potential clinical applications. *Ann Biomed Eng* 2015;**43**:3–15.
4. Kilner PJ, Yang GZ, Mohiaddin RH, Firmin DN, Longmore DB. Helical and retrograde secondary flow patterns in the aortic arch studied by three-directional magnetic resonance velocity mapping. *Circulation* 1993;**88**:2235–2247.
5. Verbeek R, Stoekenbroek RM2, Hovingh GK. PCSK9 inhibitors: novel therapeutic agents for the treatment of hypercholesterolemia. *Eur J Pharmacol* 2015;**763**:38–47.
6. Ding Z, Liu S, Wang X, Deng X, Fan Y, Sun C, Wang Y, Mehta JL. Hemodynamic shear stress via ROS modulates PCSK9 expression in human vascular endothelial and smooth muscle cells and along the mouse aorta. *Antioxid Redox Signal* 2015;**22**:760–771.

7. Adorni MP, Cipollari E, Favari E, Zanotti I, Zimetti F, Corsini A, Ricci C, Bernini F, Ferri N. Inhibitory effect of PCSK9 on Abca1 protein expression and cholesterol efflux in macrophages. *Atherosclerosis* 2017;**256**:1–6.
8. Ding Z, Liu S, Wang X, Theus S, Deng X, Fan Y, Zhou S, Mehta JL. PCSK9 regulates expression of scavenger receptors and ox-LDL uptake in macrophages. *Cardiovasc Res* 2018;**114**:1145–1153.
9. Li J, Liang X, Wang Y, Xu Z, Li G. Investigation of highly expressed PCSK9 in atherosclerotic plaques and ox-LDL-induced endothelial cell apoptosis. *Mol Med Rep* 2017;**16**:1817–1825.
10. Ding Z, Liu S, Wang X, Mathur P, Dai Y, Theus S, Deng X, Fan Y, Mehta JL. Cross-talk between PCSK9 and damaged mtDNA in vascular smooth muscle cells: role in apoptosis. *Antioxid Redox Signal* 2016;**25**:997–1008.
11. Kawasaki T, Kawai T. Toll-like receptor signaling pathways. *Front Immunol* 2014;**5**:461.
12. Matsunaga N, Tsuchimori N, Matsumoto T, Ii M. TAK-242 (resatorvid), a small-molecule inhibitor of Toll-like receptor (TLR) 4 signaling, binds selectively to TLR4 and interferes with interactions between TLR4 and its adaptor molecules. *Mol Pharmacol* 2011;**79**:34–41.
13. Kawai T, Akira S. Signaling to NF-kappaB by Toll-like receptors. *Trends Mol Med* 2007;**13**:460–469.
14. Iasiello M, Vafai K, Andreozzi A, Bianco N. Analysis of non-Newtonian effects within an aorta-iliac bifurcation region. *J Biomech* 2017;**64**:153–163.
15. Frydrychowicz A, Stalder AF, Russe MF, Bock J, Bauer S, Harloff A, Berger A, Langer M, Hennig J, Markl M. Three-dimensional analysis of segmental wall shear stress in the aorta by flow-sensitive four-dimensional-MRI. *J Magn Reson Imaging* 2009;**30**:77–84.
16. Tanaka M, Sakamoto T, Sugawara S, Nakajima H, Kameyama T, Katahira Y, Ohtsuki S, Kanai H. Spiral systolic blood flow in the ascending aorta and aortic arch analyzed by echo-dynamography. *J Cardiol* 2010;**56**:97–110.
17. Baker RG, Hayden MS, Ghosh S. NF-κB, inflammation, and metabolic disease. *Cell Metab* 2011;**13**:11–22.
18. Guijarro-Muñoz I, Compte M, Álvarez-Cienfuegos A, Álvarez-Vallina L, Sanz L. Lipopolysaccharide activates Toll-like receptor 4 (TLR4)-mediated NF-κB signaling pathway and proinflammatory response in human pericytes. *J Biol Chem* 2014;**289**:2457–2468.
19. Liu A, Frostegård J. PCSK9 plays a novel immunological role in oxidized LDL-induced dendritic cell maturation and activation of T cells from human blood and atherosclerotic plaque. *J Intern Med* 2018;**284**:193–210.
20. Liu X, Pu F, Fan Y, Deng X, Li D, Li S. A numerical study on the flow of blood and the transport of LDL in the human aorta: the physiological significance of the helical flow in the aortic arch. *Am J Physiol Heart Circ Physiol* 2009;**297**:H163–H170.
21. Van Craeyveld E, Jacobs F, Feng Y, Thomassen LC, Martens JA, Lievens J, Snoeys J, De Geest B. The relative atherogenicity of VLDL and LDL is dependent on the topographic site. *J Lipid Res* 2010;**51**:1478–1485.
22. Ylitalo R, Jaakkola O, Lehtolainen P, Ylä-Herttuala S. Metabolism of modified LDL and foam cell formation in murine macrophage-like RAW 264 cells. *Life Sci* 1999;**64**:1955–1965.

Translational perspective

Proprotein convertase subtilisin/kexin type 9 (PCSK9) regulates low-density lipoprotein receptor degradation and plays key roles in hypercholesterolaemia and related cardiovascular diseases. In this study, we show that helical flow which is associated with atherosclerosis induces more PCSK9 than linear flow. Further, pro-inflammatory cytokines directly determine PCSK9 levels. As upstream pathway, TLR4-MyD88-NF-κB signalling plays an important role in the regulation of PCSK9 expression. TRIF has almost no effect in this signalling. Thus, inhibition of TLR4-MyD88-NF-κB signalling may be a novel strategy to attenuate PCSK9 release associated with helical flow.